

Article

The Role of Past Climatic Variability in Fluvial Terrace Formation, a Case Study from River Mureş (Maros), Romania

Tamás Bartyik ¹, Petru Urdea ², Tímea Kiss ¹ , Alexandru Hegyi ²  and György Sipos ^{1,*} 

¹ Geomorphological and Geochronological Research Group, Department of Geoinformatics, Physical and Environmental Geography, University of Szeged, Egyetem u. 2-6, H-6722 Szeged, Hungary

² Department of Geography, West University of Timișoara, B-dul. Vasile. Parvan Nr. 4, 300223 Timișoara, Romania

* Correspondence: sipos.gyorgy@szte.hu

Abstract: Fluvial terrace formation is a complex process governed by the interplay of climatic and tectonic forcings. From a climatic perspective, an incision is usually related to climatic transitions, while valley aggradation is attributed to glacial periods. We have reconstructed the formation of Late Pleistocene fluvial terraces along the middle, mountainous section of a temperate zone river (Mureş/Maros) in order to identify the roles of different climatic periods and potential vertical displacement in terrace development. Investigations were based on two profiles representing two different terrace levels. The profiles were subjected to sedimentological and detailed geochronological analyses using optically stimulated luminescence (OSL). The results indicated that the investigated terraces represent different incision events coinciding with climatic transition periods. However, a joint MIS 3 valley aggradation period can be identified at both of them. Thus, the relatively mild but highly variable climate of the MIS 3 facilitated sediment mobilization from upland catchments. On the other hand, there is no evidence of aggradation under the cold and stable climate of MIS 2. However, the tectonic setting favours incision at the site. Based on our results, we concluded that the timing of the main events was controlled primarily by climatic forcing. The terrace formation model recognised might also be applied at other rivers in the region.

Keywords: fluvial terraces; OSL dating; climatic transitions; River Mureş (Maros)



Citation: Bartyik, T.; Urdea, P.; Kiss, T.; Hegyi, A.; Sipos, G. The Role of Past Climatic Variability in Fluvial Terrace Formation, a Case Study from River Mureş (Maros), Romania. *Quaternary* **2023**, *6*, 35. <https://doi.org/10.3390/quat6020035>

Academic Editors: David Bridgland, Elda Russo Ermolli and James B. Innes

Received: 13 February 2023

Revised: 11 April 2023

Accepted: 22 May 2023

Published: 2 June 2023



Copyright: © 2023 by the authors. Licensee MDPI, Basel, Switzerland. This article is an open access article distributed under the terms and conditions of the Creative Commons Attribution (CC BY) license (<https://creativecommons.org/licenses/by/4.0/>).

1. Introduction

Almost all major rivers in the Carpathian Basin display terrace systems or terrace remains. The formation of terraces is caused by changes in stream power and sediment supply, governed mostly by climatic and tectonic factors [1]. However, both generalisation and parallelization are hindered by the fact that the significance of these factors can differ from site to site [2,3].

According to the classical geomorphological approach, the formation of terraces under climatic influence is usually linked to the glacial and interglacial periods and their alternation [4,5]. Accumulation and valley fill was mainly associated with glacials, while incisions were associated with interglacials. More recently the importance of climatic transition periods is underlined [6,7]. The role of vegetation is also emphasized as it can significantly influence runoff conditions and sediment input to rivers [8]. In climatic transition periods, as a result of the time lag between climate change and the adaptation of vegetation, geomorphic processes may change relatively suddenly, thus incision and terrace formation can accelerate [2].

Terrace formation, on the other hand, can still be fundamentally influenced by tectonism, as changing relief can increase or decrease the slope of the terrain, triggering the geomorphological adjustment of the river and determining its stream power and sediment regime [5,9–11]. Tectonic movements are of different magnitudes and can be

separated spatially and temporally, thus affecting different parts of the catchment at different scales [10,12]. Moreover, as it is seen for example along the Hungarian section of the Danube, tectonic uplift was responsible for the vertical differentiation of terrace sediments rather than for the formation of terrace levels [5,13].

Consequently, terrace formation can usually be determined by the interplay of these main governing forces [5,14]. More precisely, the general trend of change is maintained by tectonic movements, but the trend can be overridden from time to time by the oscillation of climate and fairly abrupt geomorphic processes related to climate change. Still, it remains a challenge in each case to determine the magnitude and importance of climatic and tectonic forces. It has been shown previously that regional and catchment controls may interact with global climate forcing on strath formation [15]. Catchment scale controls can comprise vegetation, rock type, glacial proximity, and precipitation patterns. These exert a first-order control on sediment supply and transport capacity, which govern then reach scale aggradation and incision; i.e., river style depends on the ratio of sediment flux to river discharge [16–18]. This ratio emphasizes the need to investigate basin-specific landscape response to climate change.

On its lower reaches, the course and the dynamics of River Mureş (Maros) are determined predominantly by the continuous subsidence of the Lower Tisza Graben [19], and on its upper reaches by the differential uplift of mountain ranges surrounding the Transylvanian Basin [20,21]. Along its course from the Transylvanian Basin to the Great Hungarian Plain, the river has followed the tectonic line between the Southern Carpathians and the Apuseni Mountains, at least since the Upper Pliocene [22]. Early research of [23] and [24] separated three terrace levels along this section, belonging to the Early Holocene, Upper, and Lower Pleistocene. Later, [20] and [25] identified five terrace levels, which were attributed to the alpine glaciations Günz, Mindel, Riss, Würm, and the Upper Pliocene. According to [26], the oldest three terrace levels have hardly survived due to erosion, and terraces at a 20–30 m height are actually Würm forms, resulting in an almost continuous flat area almost along the entire valley. Compared to previous authors, a somewhat more detailed classification has been proposed by the Harta geologică a R. S. România, Deva sc. 1:50,000 map, where terrace levels are classified based on their relative altitude above the present floodplain. This way, eight terraces can be separated, though age is not provided.

The identification and dating of terrace levels along the Mureş (Maros) are also complicated by the fact that different generations of terraces have reached different heights through post-genetic tectonic movements. This problem is partly resolved by classifying them into height categories, as done by Harta geologică a R. S. România, Deva; however, this categorization may also hide temporal differences concerning their formation. On the other hand, considering the model related to climatic transitions might lead to recording numerous events by the Mureş (Maros) terrace system, which also contributes to the difficulty of fluvial reconstruction. The numerical age control of fluvial terrace deposits is generally poor in the area, and age estimates are mainly based on lithostratigraphy and the height of terraces above the modern floodplain.

Optically stimulated luminescence (OSL) is used widely in dating the formation of almost any sedimentary deposits, including fluvial terraces, e.g. [13,27,28]. However, the use of OSL can be limited by incomplete bleaching, typical during low light fluvial transport processes, and especially characteristic in terms of the fine grain, suspended part of fluvial sediments [29,30]. Considering the mineral grains used routinely for dating, incomplete bleaching affects quartz less than feldspars, as the former needs a much shorter time for signal resetting under natural light conditions. Consequently, coarse-grain quartz should be preferred for dating fluvial deposits, although its use is limited by the fact that it saturates relatively early and allows OSL dating back to 40–50 ka, in general, as indicated by [31].

Considering the above, the primary aim of the present study was to date the formation of the 5–10 m multiple terrace levels of the Mureş (Maros) River at Deva, Romania, and to assess how they can be related to the climatic transition model of terrace development. The results obtained can contribute to the more detailed evaluation of fluvial processes

in the valley of the river and may also help in the interpretation of other Late Pleistocene terrace forms in the region and beyond.

2. Materials and Methods

2.1. Study Area

The study area is situated on the lower part of the upland catchment of the nearly 750 km long Mureş (Maros) River, the largest tributary of the Tisza River. The area of the Mureş (Maros) catchment is ~30,000 km². The river collects water from the inner slopes of the Eastern and Southern Carpathians, the Transylvanian Basin, and the Apuseni Mountains. The present mean discharge of the river on the basis of long-term data from Alba Iulia and Arad is 140–150 m³/s [32]. However, paleochannels further downstream on the Mureş (Maros) alluvial fan indicate periodically higher magnitude of discharges in the past [33]. Some parts of the catchment, especially the Retezat Mountains, were glaciated in glacial periods. The proportion of these areas compared to the entire area of the catchment is low, and deglaciation did not contribute considerably to lowland discharges [34]. The channel sediments are dominated by coarse sand and fine gravel at the study site; however, the river also carries a large amount of suspended sediment, eroded mostly along its way through the Transylvanian Basin.

In the study reach, the river flows along the tectonic contact of the Apuseni Simici Sheets and the Supragetic Domain of the Southern Carpathians, which is the eastward continuation of the G7 fault of the Pannonian Basin [35]. The petrographic and structural heterogeneity of the Deva corridor is proved by significant gravimetric differences [36], which also explain the seismicity in the area of Deva at magnitudes between three and five. The uplift rate is not known, but recent vertical crustal movements have values between +1 mm/year in the E and –1 mm/year in the W part of this sector [37].

The average slope of the channel is 51 cm/km along the study reach, but partly due to tectonic control and geomorphic forcing, the slope is highly variable. Three distinct sections can be separated (Figure 1). The upstream section has a slope of 85 cm/km, which drops suddenly to 16 cm/km from the confluence with River Strei. This tributary drains the highest elevation, most glaciated sub-catchment of the entire watershed. Consequently, the Strei deposited an extensive alluvial fan and filled up the valley of the main river here. The next section, with a 52 cm/km slope, starts downstream of a valley bottleneck, appearing due to petrographic changes. The high sediment input and the narrowing of the valley, along with vertical displacement, provided ideal conditions for fluvial terrace formation in the past.

The investigated terraces are located NW of the city of Deva between 300 and 310 river km, where the valley of the river narrows from 4–5 km to 1–2 km. Along this reach, several terrace forms were identified previously, and the investigated terrace surfaces are classified in the 5–10 m category according to the Harta geologică a R. S. România, Deva sc. 1:50,000 (Figure 1).

The two terraces investigated are situated on opposite sides of the river, and the distance between them along the valley is only 2 km. The difference between their relative altitude above the present-day floodplain is 4–5 m. The higher terrace, situated upstream on the right bank of the river, has an absolute height of 190–192 m asl. Both on its eastern and western ends, small subsequent tributaries (Certej Stream and Boholt Stream) first built their small alluvial fans, then incised by headward erosion (Figure 1). The lower downstream terrace, with an absolute height of 186–188 m, is located on the left bank of the river.

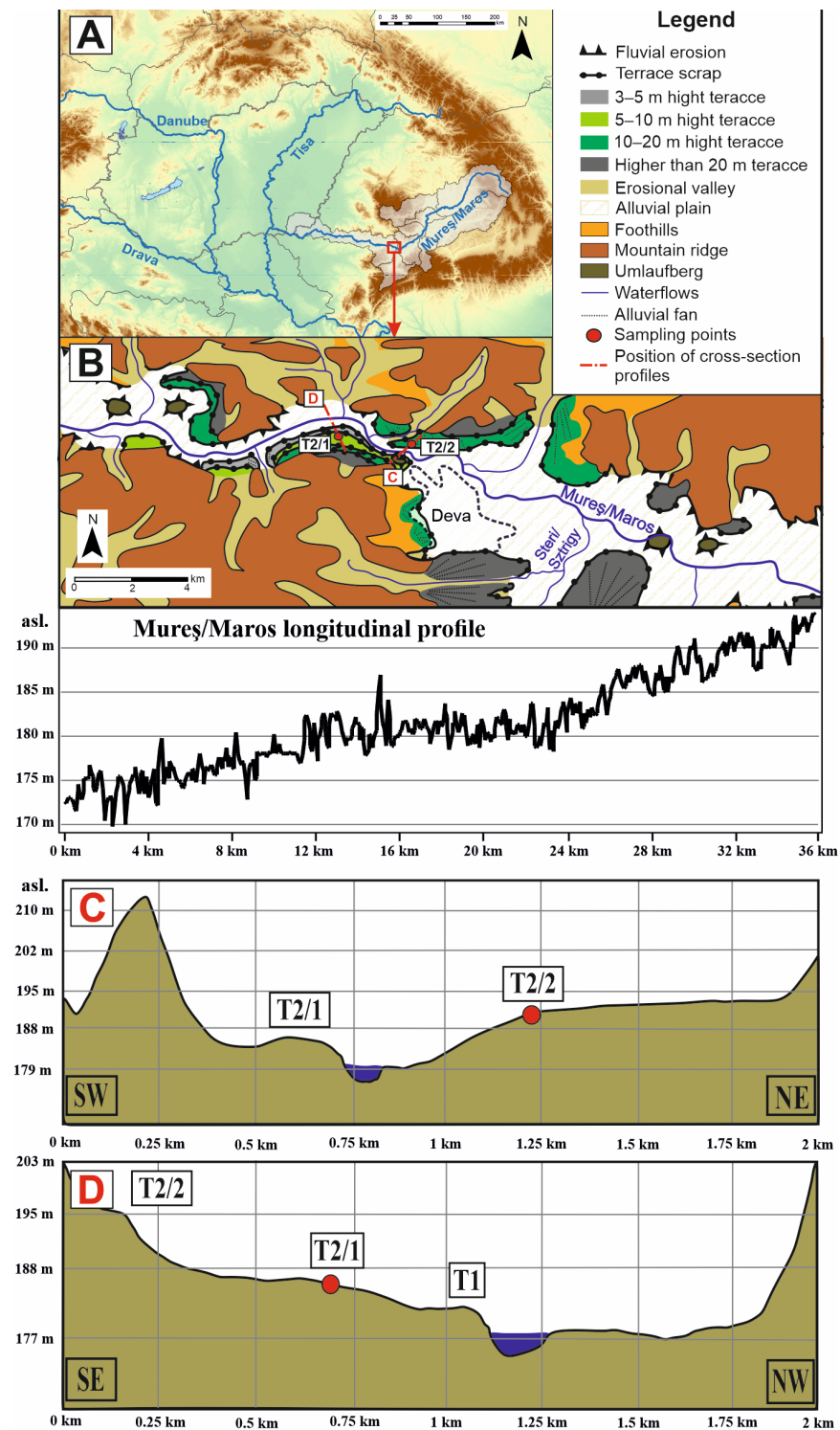


Figure 1. (A) Location and geomorphological setting of the study area. (B) The longitudinal profile of the river along the study area. (C,D) Valley cross-sections with identified terrace surfaces.

2.2. Sampling and Sedimentological Analyses

Terraces were identified on the basis of the EU-DEM digital elevation model, field visits, and the geological map of Harta geologică a R. S. România, Deva sc. 1:50,000. In the case of terrace T2/2, sampling was made at a road cut, exposing the scarp of the terrace. The upper part of the section, however, could only be sampled by drilling, using an Eijkelkamp-type hand corer and a kit for undisturbed sampling. Two layers down to a depth of 2 m

were sampled for OSL and grain size analysis, as a highly compacted clayey layer was hit. Following a 3 m gap, the remaining samples were collected from the exposure by hitting steel cylinders into the layers of the gravelly-sandy upward fining sequence. The bedding layer, composed of coarse gravel, was not sampled, as it contained no suitable material for dating. In total, seven OSL samples were collected at this.

Since no exposures were found on the field at terrace T2/1, sampling was made exclusively by drilling. The borehole could be drilled down to 2.1 m from the surface, where gravelly (2–5 cm) sand was found, in which further drilling was not possible. At this site, two OSL samples were taken from the two layers identified.

Profiles were described macroscopically on the field, and grain size samples representing each layer were analyzed using a Fritsch MicroTech Analysette 22-type laser analyzer (FRITSCH, Idar-Oberstein, Germany) to make macroscopic description more precise by considering the D_{50} and D_{90} values obtained. The maximum grain size that can be measured with the device is 2000 μm . However, in the case of terrace T2/2, the section below 540 cm contained several pieces of gravel and grains, which were larger than the measurable grain size. Therefore, in the case of terrace T2/2, the grain size distribution of the section below 540 cm could only be examined by sieving (Figure 2).

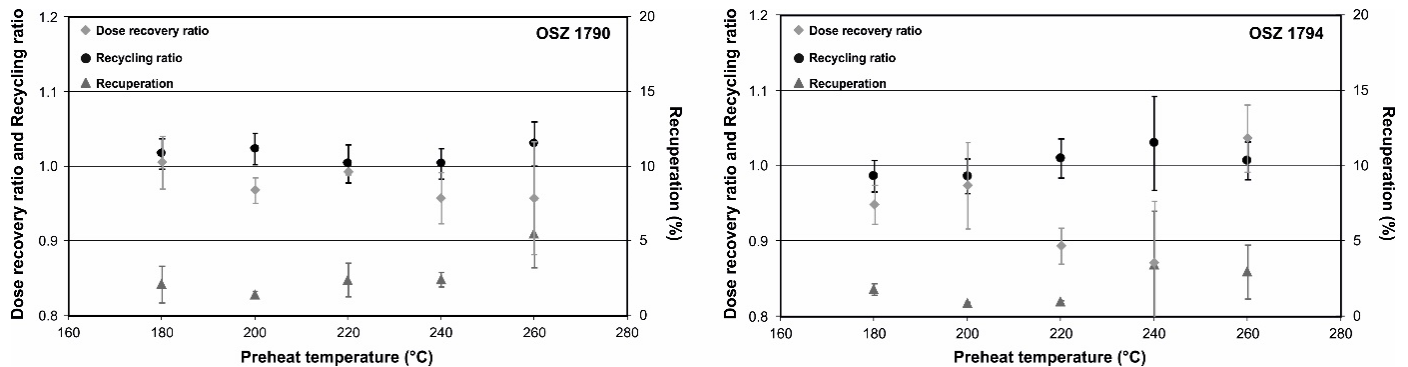


Figure 2. Combined preheat and dose recovery test results for samples OSZ 1790 and OSZ 1794.

2.3. Luminescence Dating

Samples were removed from sampling cylinders in the laboratory under the yellow light of low-pressure sodium lamps. Sample preparation followed the usual steps advised, e.g., [38,39]. After measuring their wet weight, each sample was dried. Based on their dominant grain size (sand or silt), samples from different layers were processed in different ways. In the case of silts, the fine-grain technique was applied, and the 4–11 μm fraction was separated by settling in Atterburg cylinders. In the case of sands, the coarse-grain technique was applied, and potential fractions for measurement (90–150 μm , 150–220 μm , and 220–300 μm) were separated by sieving. Preparation was continued on the largest grain size fraction yielding a reasonable amount (a few grams) of material. Thus, the selected grain size differed from sample to sample.

Both fine and coarse-grain samples were treated with 10% hydrochloric acid (HCl) and 10% hydrogen peroxide (H_2O_2) for carbonate and organic material removal. Due to its favorable properties and the expected age range of the samples, quartz was selected for OSL measurements. The 4–11 μm fraction was subjected to a one-week treatment in hexafluorosilicic acid (H_2SiF_6) to etch feldspars and to enhance the abundance of quartz in the samples. In the case of coarse grain samples, density separation, and subsequent 40 min 40% hydrogen-fluoride (HF) treatment were applied to prepare pure quartz extracts. For the measurements, several aliquots were prepared from each sample by mounting fine and coarse grain samples on 10 mm \varnothing aluminum and stainless-steel discs, respectively.

Under fluvial conditions, OSL age calculated from fine grain samples (4–11 μm) may lead to considerable age overestimation [30,40]. This phenomenon is caused by inadequate bleaching of sediment grains, being more significant in terms of silty sediments. For this

reason, in the case of the silty samples, we also tried to obtain coarse grain extracts. This could only be achieved in the case of three samples and only by separating a wide range of sand-sized grains (90–300 μm). For these samples, measurements were performed on the silty and the sandy fractions as well. Since even coarse-grained samples can be affected by inadequate bleaching in a fluvial environment, single-grain measurements were also performed to test potential age overestimation in the case of one suitable sample with high luminescence sensitivity.

The OSL age of samples is given as the ratio of the absorbed total radioactive dose since deposition, termed equivalent dose " D_e ", and radioactive dose produced in the surroundings of the sample in unit time, termed dose rate " D^* ". The D_e of quartz samples was determined using a RISØ TL-DA-20 luminescence reader, applying the single aliquot regeneration (SAR) protocol [41]. Prior to the equivalent dose measurements, a combined preheat and dose recovery test was performed on two selected samples from the two profiles in order to determine the most appropriate measurement parameters.

Several small aliquots were used during the multigrain measurements to determine sample D_e values, which were statistically evaluated using either the minimum (MAM) or the central age model (CAM) [42]. The decision on which age model had to be applied was made on the basis of the dispersion, skewness, and kurtosis of dose distributions [43]. Single aliquot dose values were plotted on abanico plots using the RStudio "Luminescence package" [44]. In the case of the additional single-grain test, 96 grains were mounted separately on stainless steel discs. Measurements were made in the same multi-grain system using the same measurement and evaluation procedures described above.

Samples were also examined by linearly modulated optical stimulation (LM-OSL) to resolve the components of the OSL signal and to determine the ratio of the fast component [45,46], which was used as an indicator of the so-called luminescence sensitivity of quartz grains. Luminescence sensitivity is the signal intensity measured per unit dose, which recently proved to be a useful parameter for provenance analysis, e.g., [47,48]. LM-OSL measurements were made on previously weighed and bleached aliquots receiving an identical 24 Gy β -dose. The same RISØ equipment was used for each measurement. Stimulation lasted for 1000 s, during which LED power was increased linearly up to 90% of the maximum intensity.

The environmental dose rate was determined using gamma spectrometry by measuring the concentration of ^{238}U , ^{232}Th , and ^{40}K in the sediment samples surrounding the OSL samples. The sediment samples were first dried, crushed, and placed in 450 mL Marinelli beakers, then stored for at least 21 days to allow ^{222}Rn to build up and get in equilibrium with ^{226}Ra . Measurements were made using a high-purity Canberra XtRa Coaxial Ge detector. The specific activities of radionuclides were converted to dry dose rates using the conversion factors of [49]. Wet dose rates were calculated on the basis of the in situ water content of the samples. The cosmic dose rate was determined from the geographical position and the depth of the samples according to [50].

3. Results

3.1. Luminescence Properties

The combined preheat and dose recovery test was performed on sample OSZ 1790 from terrace T2/2 and on sample OSZ 1794 from terrace T2/1 (Figure 2). In the case of the first sample, important SAR criteria were in the desired range (recycling ratio = 1.0 ± 0.1 ; recuperation < 5%), and dose recovery ratios were close to unity up to a preheat of 240 °C; above this temperature recuperation, the error of recycling and dose recovery ratios significantly increased. In terms of sample OSZ 1794, the analyzed parameters remained adequate only at lower preheats, and errors, as well as recuperation, started to increase from 220 °C (Figure 2). Based on the tests, the temperature range between 200 °C and 220 °C proved to be the most adequate for D_e determination. Consequently, a 210 °C preheat was applied for subsequent SAR measurements.

With the use of LM-OSL, six OSL components—one fast, one medium, and four slow—could be resolved in seven out of the eight samples analyzed from terrace T2/2. In the case of one sample (OSZ 1791), five components were identified (Figure 3). No ultrafast component was found in any of the samples, and in the initial part of the signal, the dominance of the fast component was inevitable (Figure 3). Nevertheless, the intensity of the fast component relative to the overall signal, i.e., the fast component ratio, shows considerable differences from sample to sample. Sample OSZ 1793 exhibited the lowest (3%), and sample OSZ 1790 had the highest (7%) value in this respect. On average, the ratio of the fast component was 5% in the case of T2/2 samples.

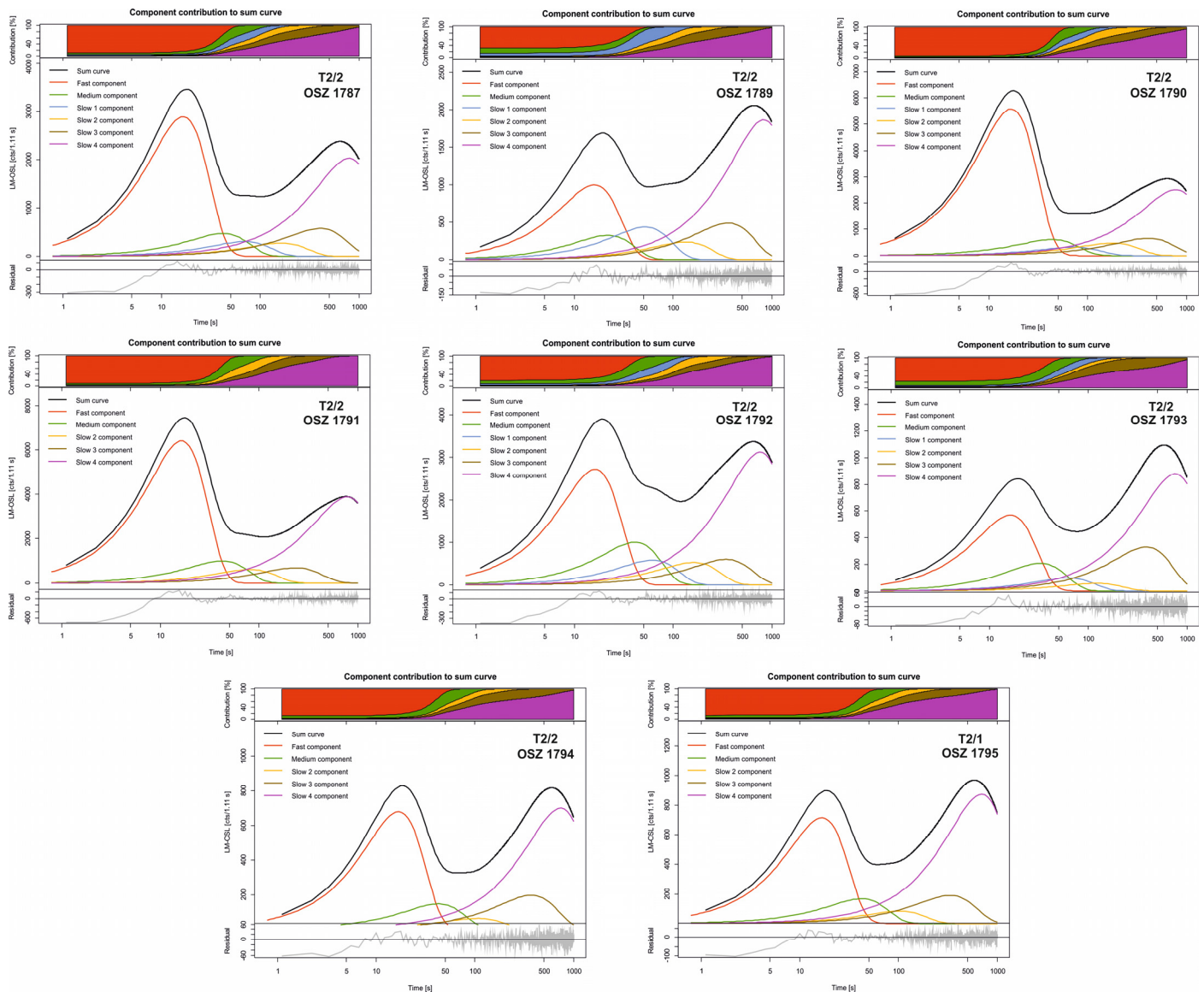


Figure 3. Resolved OSL components for representative aliquots of the samples.

In total, five—one fast, one medium, and three slow—OSL components could be separated in the two samples of terrace T2/1. The initial signal is also dominated by the fast component, but its proportion was 3% in both samples. This is similar to the value seen in terms of sample OSZ 1793, collected from the other terrace. In all, the composition of the OSL signals also made these sediments suitable for OSL dating.

Single-grain measurements were performed on the most sensitive sample (OSZ1792). In total, 18 out of 96 grains yielded reasonable, natural, and regenerated luminescence signals to calculate D_e values, though dose errors were above 10% in many cases (Figure S1).

The calculated single-grain age (33.9 ± 3.1 ka) was 11% lower than the multi-grain age (38.0 ± 2.7 ka); however, the error bars of the two results overlap. Consequently, there is a potential but not significant age overestimation concerning multi-grain measurements. Moreover, as most of the samples are highly insensitive, the prepared small aliquots (100–200 grains/disc) carried only a few bright grains, meaning that multi-grain D_e estimates should yield similar results as single-grain measurements.

Based on the comparative measurement of fine and coarse grain fractions of certain samples (OSZ 1789 and OSZ 1794), it can be seen that the fine grain fraction gives higher ages; i.e., incomplete bleaching probably overestimates the true deposition age of silty samples (Table S1). However, in the case of sample OSZ 1787, the two different fractions yielded ages within error limits. This result is probably due to slow and repeated sediment transport that resembles a lower energy environment than in the case of the deposition of other samples [39,51]. In terms of sample OSZ 1788, composed of silt and not containing sand, no comparison could be made between fractions. However, based on the stratigraphic sequence of ages, the reported fine-grain age is certainly an overestimation. Consequently, this sample was not considered during the evaluation of the results.

3.2. Stratigraphy and OSL Ages of Terrace T2/2

At profile T2/2, the coarse grain gravel terrace material can be identified 640 cm below the terrace surface, i.e., approximately 5 m above the altitude of the present-day floodplain. The gravel pieces have a size of 5–10 cm, similar to the maximum size of gravel pieces in the present-day channel. Thus, the layer presumably represents the surface of an in-channel bar (Figure 4). This layer is covered by a 60 cm thick, light greyish color, upward fining sand deposit ($D_{50} = 76 \mu\text{m}$, $D_{90} = 249 \mu\text{m}$) that is rich in phyllosilicates and contains gravel pieces of 2–5 cm but without any signs of cross-bedding. As two thin silt stripes can also be identified, this unit is interpreted as a trough fill. The OSL age of the deposit is 36.4 ± 2.5 ka, and the normalized sensitivity of the OSL fast component is 174 ± 50 cts/mg/Gy (Table S1).

From 540–570 cm, a cross-bedded greyish sand layer can be found. This layer is characterized by a finer grain size than the previous one ($D_{50} = 32 \mu\text{m}$, $D_{90} = 80 \mu\text{m}$). However, it contained small 1–2 mm clasts and 2–3 cm blocks of compacted and rounded silt, while the number of phyllosilicates was considerably less. All these refer to a different source of the material, which is also indicated by the considerable change in luminescence sensitivity (870 ± 217 cts/mg/Gy) compared to that of the sediments below (174 ± 50 cts/mg/Gy). Consequently, this deposit might be attributed to the Boholt Stream and interpreted as its alluvial fan deposit, intercalating Mureş (Maros) River sediments. Two OSL samples were taken from this unit, and the ages obtained (38.0 ± 2.7 ka and 36.8 ± 3.1 ka) are very close to that of the preceding layer. The cross-bedded deposit is covered by a greyish pack of medium to fine sand ($D_{50} = 47 \mu\text{m}$, $D_{90} = 139 \mu\text{m}$), fining upwards in general with the exception of a relatively coarse layer at a depth of 520 cm ($D_{50} = 41 \mu\text{m}$, $D_{90} = 194 \mu\text{m}$). This sediment layer was laid at 33.6 ± 1.9 ka, and based on OSL sensitivity values, it can also be related to the depositional activity of the stream.

From around a depth of 500 cm, a lower energy fluvial environment can be reconstructed, as sediments above in the profile are rather silty or even clayey. The sand of the Boholt Stream is covered by a brownish silt deposit, of which only 30 cm was accessible in the exposure. The age of the sandy silt is 26.1 ± 2.2 ka, and the OSL sensitivity of quartz grains gets considerably lower (410 ± 71 cts/mg/Gy). As such, this part of the sequence can possibly be related again to the Mureş (Maros) and can be interpreted as an overbank deposit of the river.

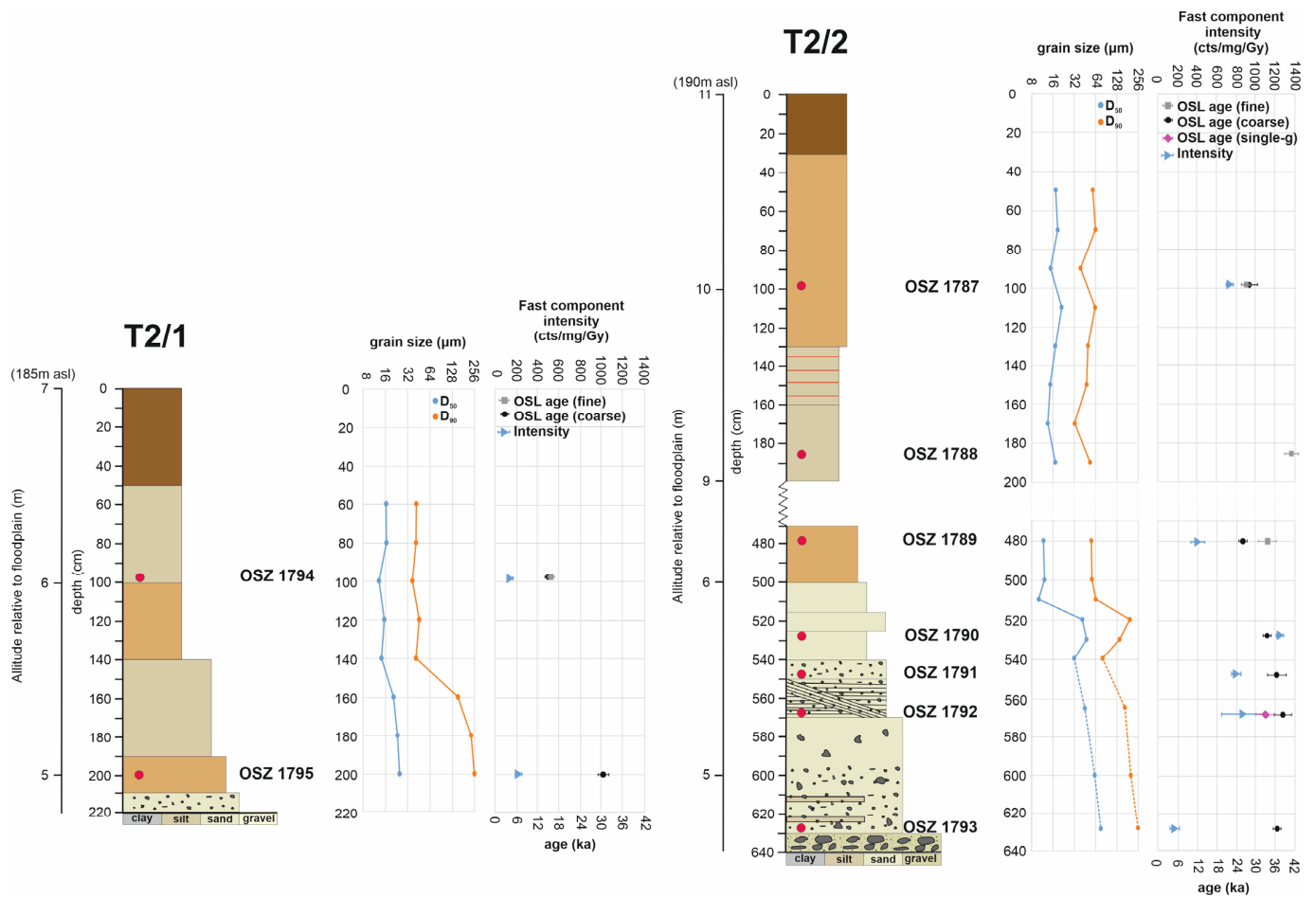


Figure 4. Stratigraphy of the investigated terraces, mean grain size values, OSL ages, and luminescence sensitivity values.

Although 3 m of the sequence could be accessed neither in the exposure nor by drilling, based on the samples recovered from above, it seems that the low energy environment could prevail until the intensive incision started. From the maximum depth of the drilling, approximately 9 m above the present-day floodplain, to a depth of 130 cm from the surface, a greyish, clayey silt layer ($D_{50} = 13 \mu\text{m}$, $D_{90} = 32 \mu\text{m}$ at a depth of 170 cm) can be identified with thin accumulations of iron oxides. The age of the overbank deposit could not be precisely identified as no coarse-grain quartz was available from the OSL sample. Therefore, the upper part of the sequence can be dated using the sample obtained from a slightly coarser silty deposit above, which contained an adequate amount of sand for dating. The age of the sample, collected at a depth of 100 cm, was $28.7 \pm 2.5 \text{ ka}$, which is very similar to that of the sediment at the top of the exposure (OSZ 1789). Consequently, a relatively high deposition rate can be presumed for this period. The OSL sensitivity of the topmost sample rises again ($753 \pm 22 \text{ cts/mg/Gy}$), though it does not reach the values measured at a greater depth. Still, the quartz grains in this layer can likely be related again to the depositional activity of the Boholt Stream.

3.3. Stratigraphy and OSL Ages of Terrace T2/1

At site T2/1, sediments could only be investigated through drilling. Consequently, the coarse gravel layer found at section T2/2 could not be identified in this case directly. However, at a depth of 220 cm, an unbreakable layer of sandy gravel was hit, with a similar character to that found at the other site at a depth of 600 cm. The drill head brought up 1 cm diameter gravel pieces. Moreover, the two layers were found at a very similar relative elevation with respect to the present-day floodplain. Consequently, they

presumably represent the same depositional event. OSL sampling could only be carried out from the layer above, composed predominantly of medium silt but still rich in medium sand containing phyllosilicates ($D_{50} = 25 \mu\text{m}$, $D_{90} = 251 \mu\text{m}$). Not only the composition of the sandy fraction but the value of quartz OSL sensitivity ($203 \pm 25 \text{ cts/mg/Gy}$) also refers to a Mureş (Maros) related origin in this layer. The OSL age of the cover sediment ($30.5 \pm 1.2 \text{ ka}$) is 5–6 ka lower than the age obtained from Mureş (Maros) sediments at the bottom of profile T2/2. Based on this information, a hiatus is suspected at the interface of gravelly and silty sediments in profile T2/1.

Above the sandy silt layer, a transitional, upward fining, light brown silty deposit is situated with a considerable amount of mica, indicating decreasing energy floodplain sedimentation. This layer is followed by a slightly browner silty horizon ($D_{50} = 15 \mu\text{m}$, $D_{90} = 45 \mu\text{m}$), still rich in phyllosilicates but referring to an initial stage of soil formation. The second OSL sample from this sequence was collected from a depth of 1 m, near the border of the brown horizon and a light grey, brownish, 50 cm thick overbank deposit above ($D_{50} = 16 \mu\text{m}$, $D_{90} = 46 \mu\text{m}$). The age of the sample indicates the return of floodplain sedimentation at a considerably later period ($14.8 \pm 0.8 \text{ ka}$) than expected, considering the ages obtained so far from the two investigated profiles. Based on the measured OSL sensitivity value of the sample ($157 \pm 14 \text{ cts/mg/Gy}$), the deposit fits the low-sensitivity sediments of the Mureş (Maros) River, confirming that the layer had been deposited by the river itself.

4. Discussion

4.1. Reconstruction of Terrace Development with a Climatic Approach

Based on coarse grain channel sediments recovered from a very similar altitude at both sites and the experienced similarity of OSL fast component sensitivity, findings indicate the two investigated terraces belong to the same deposition cycle of the Mureş (Maros) River. However, the altitude difference of their surfaces and the difference in OSL ages obtained for overlying sediments show that they resemble separate phases of the incision. Consequently, both investigated terraces are fill terraces, and T2/1 is nested into T2/2.

The age of the coarse gravel deposit recovered at terrace T2/2 could not be determined directly due to the lack of sand-sized grains. However, sand and fine gravel layers immediately above this deposit, which were identified in both profiles at an approximate height of 180 m asl, provided a deposition age between 38 and 30 ka (Figures 4 and 5), indicating extensive aggradation in the valley until the end of MIS 3 (Figure 5). Although climatically relatively milder as indicated by soil formation in the loess records of the region [52], the MIS 3 interstadial nevertheless pointed to cold, sometimes periglacial conditions in Central Europe [53]. However, on the lowlands of the Carpathian Basin, steppe vegetation was mostly characteristic [54]. MIS 3 can also be characterized by a more pronounced seasonality in the entire Northern Hemisphere [55] and also in the region [54], thus explaining the initiation of sediment pulses towards the Mureş (Maros) Valley from the glaciated regions of the catchment [34] and the aggradation of a significant valley fill in spite of potential tectonic forcing at the site.

For the cold periods, the existence of permafrost in the vicinity of the glacial morpho-climatic domain should not be excluded [53]. The warming, specific to the interglacial stages, determined the degradation of the permafrost and the acceleration of the dynamics of the slopes, which also influenced the dynamics of the sediments in each hydrographic basin. Similar MIS 3 coarse grain terrace deposits were identified at other European rivers lately, e.g., at the lower reaches of the Tejo River, where base-level change, i.e., sea level rise and increased sediment availability were identified as the driving factors of gravel deposition [56]. In an Alpine foreland setting, a major phase of aggradation with a braided channel pattern was found at 40–50 ka on River Weser, as well [57]. However, the spatially closest study identifying a significant MIS 3 valley aggradation phase is that of [58] who found that climate was the dominant driver of terrace formation in the Tatra Mountains, Northern Carpathians. A similar phenomenon, though in relation to interglacial rather than

interstadial periods, is reported by several authors identifying a climatic forcing behind terrace development, see e.g., [58–61]. The previous examples and the present findings also highlight the significance of milder periods during glacial periods with the aggradation of river valleys and the formation of subsequent terrace deposits.

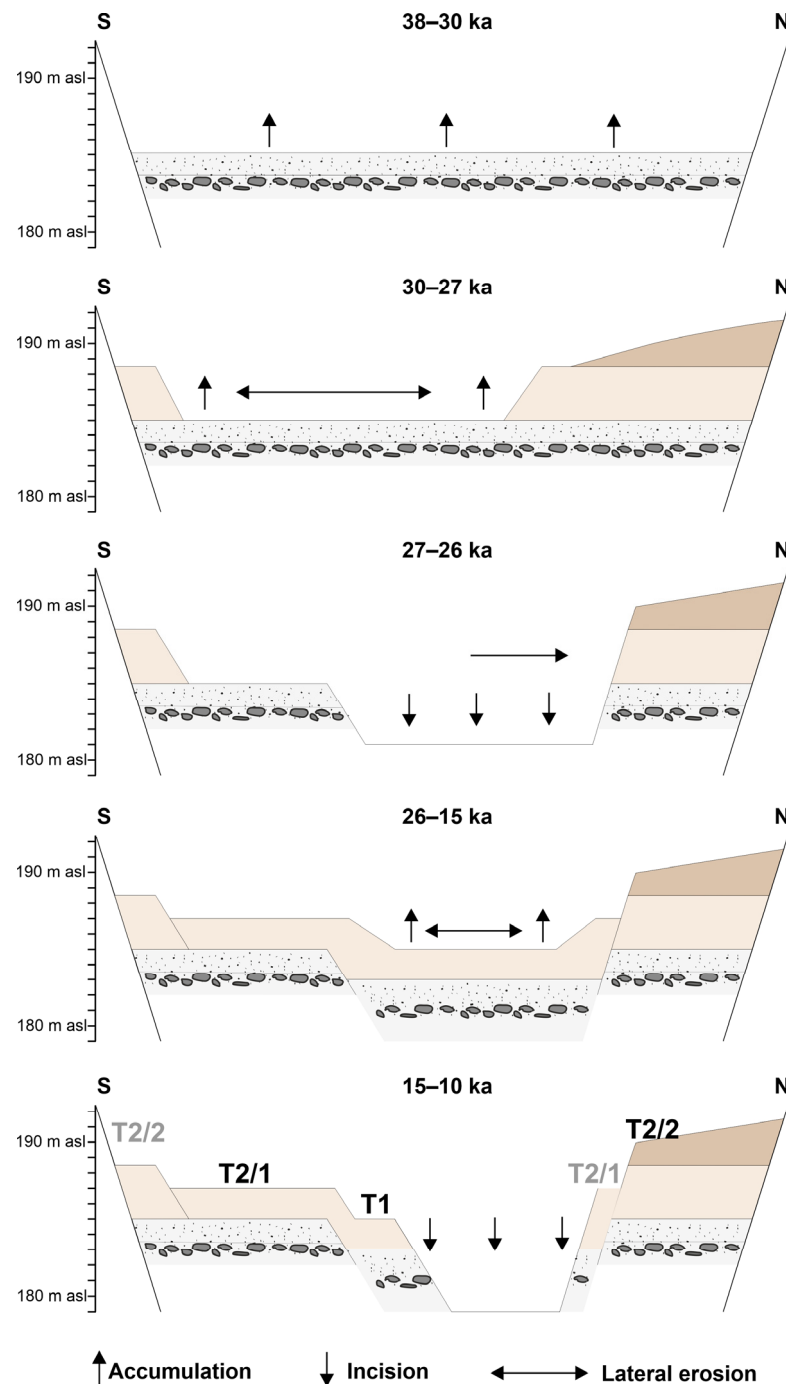


Figure 5. Reconstructed terrace development in the study area.

The presence of an upward fining overbank sequence above the channel deposits at site T2/2 indicates medium energy floodplain development between 30 and 27 ka, supplemented by additional sediments arriving from small subsequent valleys (Figure 5). However, by the end of the period, coinciding with the climatic transition between MIS 3 and MIS 2, a considerable incision started (Figure 5). Applying the general model of climate forcing, this incision can be explained by increased runoff due to decreasing

evapotranspiration as a consequence of climate deterioration and decreasing vegetation cover, see, e.g., [62–64].

However, warm-cold transition periods are less prone to initiate downcutting in comparison to cold-warm transitions [15,63,65], so the role and interplay of at least two other factors must be considered here: the availability of sediments on the catchment and the effect of tectonic processes (expanded later). As stated by [15], rivers in a temperate climate are usually supply-limited during glacial periods, which can only change during MIS transitions. This phenomenon leads finally to incision. In this general model, warm-cold events can be explained by the extensive interglacial mobilization of deposits, significantly decreasing the availability of coarse grain sediments during the transition period [59,61]. A similar process was unveiled at the NE Tibetan Plateau in the Qilian Shan by [66], where they found that incision in the uplifting region occurred systematically during warm-cold transitions, such as the MIS 3/2 at 26 ka. The finding led to the conclusion that downcutting is more sensitive to the decrease in sediment flux than to the increase of water discharge, an outcome also supported by studies on other tectonically active areas [16,17] (Figure 5).

Sediment availability at the Deva terraces is significantly controlled by the left bank tributaries of the Mureş (Maros) River near the site (Figure 1), which bring coarse grain sediments directly from the Retezat and Sureanu Mountains, the most elevated parts of the entire catchment and heavily glaciated during the LGM [67,68]. As other, more upstream parts of the catchment were not glaciated, the sediment flux to river discharge ratio could decrease significantly and can explain the start of incision at the sites from around 27 ka (Figure 5).

Moderate sediment supply probably persisted throughout the MIS 2 in the river system, but since precipitation became significantly lower in the LGM [53,68,69], the discharge of the Mureş (Maros) and its tributaries also decreased. Still, based on the studied profiles, it seems that aggradation, usually attributed to this period in the general climatic model of terrace development [15,70], was limited to the bottom of the previously incised valley (Figure 5). Nevertheless, clear evidence in the sedimentary record of site T2/1 suggests that during the Late Glacial Period, overbank deposits buried MIS 3 sand on the left bank (Figure 5). By this time, therefore, the incised valley was partly filled up again (Figure 5). The 14.8 ± 0.8 ka OSL age obtained from the sandy fraction of the silty deposit at site T2/1 might suggest linking the aggradation again to a warm period, this time the Bølling-Allerød Interstadial, and subsequent incision to the GI1/GS1 warm-cold transition (Figure 5). However, such a conclusion would require further sampling at the high and low floodplain levels of the river.

It also has to be kept in mind that compared to MIS 3, the Bølling-Allerød and later the Holocene periods were warm and humid; thus, the mobilization of LGM deposits is recorded by subsequent sediment pulses on the alluvial fan of the river [34,71]. Due to the fast response of vegetation to warming [54], the system could reach a supply-limited state again but in an interstadial and interglacial climate, conditions which inevitably favor incision (Figure 5). Therefore, the present data do not allow for an unambiguous explanation of incision around, or after, 15 ka, especially because, according to [72], even under the more responsive climate of Western Europe, Late Glacial variations were not able to change the style of rivers.

4.2. The Potential Role of Tectonic Forcing

Nevertheless, another potential factor for incision, i.e., tectonic forcing, must also be considered, since in a similar setting in the SE Carpathians [73] found that terrace formation is primarily controlled by the uplift of the mountain chain. In addition, downstream of the investigated terrace sites, a knickpoint can be identified (Figure 1), revealing vertical displacement in the lack of significant lithological changes along the longitudinal profile of the Mureş (Maros) River Valley at the studied section.

A temporal change in the displacement and the repeated upstream progradation of the knickpoint could also explain the separation of different terrace levels at the site. A key problem with this explanation is that tectonic uplift rates are difficult to derive independently from incision rates recorded by river terraces [70]. Furthermore, the changing rate

of vertical displacement in the long run can lead to terrace formation by itself mostly in slowly deforming regions [74,75], whereas, in actively and intensely uplifting areas from the Tibet Plateau [76] to the Andes [77], terrace ages fit mostly to climatic oscillation, and cannot simply be explained by changes in uplift rates. A similar conclusion was made by [58] regarding the Northern Carpathians.

Further research on the middle catchment of the Mureş (Maros) also suggests that climate have modified and influenced geomorphological processes on a large scale in this area [34,78]. The Râul Mare valley of the Retezat Mountains in the Southern Carpathians and the Hateg Basin in the foreland of the locality underwent the coarse-grained accumulation seen in the terraces during the late MIS 3 (38–30 ka), while more extensive incisions may also have taken place over a similar time interval during climate transitions [34,78].

Joint results show that major accumulation and erosion activities occurred in approximately the same period in different areas of the Mureş (Maros) catchment. Given that these periods coincide with climatically variable or transitional periods, it can be concluded that the observed processes are most likely to be primarily climatically driven. Consequently, in the given timeframe of the study, i.e., the past 30 ka, it is clear that tectonic displacement could not accelerate or decelerate at such rates that it could overrule climate and sediment supply-controlled processes at the studied site. Accordingly, it remains true that the general tendency of incision is governed by tectonics, but the rate of change in many cases will not explain the formation of straths or cut-fill terraces.

5. Conclusions

The quartz fraction of each sediment sample was suitable for OSL dating, as it was proved by preheating, dose recovery tests, and the LM-OSL fast component ratio of samples. Age overestimation of the fine grain (4–11 µm) fraction was significant in comparison to coarse grain (90–300 µm) derived ages. Sediments on the top part of terrace T2/2 showed a luminescence sensitivity two-and-a-half times stronger than that of the other samples, indicating a different sedimentary source in their case.

Based on OSL ages, sedimentological and luminescence properties, the investigated terrace levels can be attributed to the same terrace formation period. Intensive coarse-grain sedimentation, i.e., valley-filling can be dated to the end of MIS 3 (40–32 ka) in the middle section of the Mureş (Maros) River. Similar observations can be made on other European rivers, as well. Concerning the Mureş (Maros) River, increased fluvial incision events were identified at the milder to cold MIS 3/MIS 2 (~30–27 ka) and the cold to warm GS1/GI1 (~14 ka) transitions, in line with general climate change-related terrace incision models. Furthermore, sediment availability and sediment transport capacity were in equilibrium in the area during MIS 2.

The results show that the major periods of valley aggradation are related to relatively mild and climatically highly variable periods, when sediment production was high, and increased discharges could also occur. On the other hand, an incision is related to more climatic shifts. This observation means that although the tectonic setting favors incision at the site, the timing of the main events was controlled primarily by climatic forcing. This model of terrace development should be tested in the future on other temperate zone rivers, as well.

Supplementary Materials: The following supporting information can be downloaded at: <https://www.mdpi.com/article/10.3390/quat6020035/s1>, Table S1: Summary of OSL results. Figure S1: Abanico plot of single grain quartz equivalent dose values for sample OSZ 17892.

Author Contributions: Conceptualization, G.S., T.B. and T.K.; methodology, T.B. and G.S.; software, T.B. and A.H.; validation, P.U. and A.H.; formal analysis, T.B.; investigation, T.B. and G.S.; resources, G.S.; data curation, T.K.; writing—original draft preparation, T.B. and G.S.; writing—review and editing, G.S., P.U. and T.B.; visualization, T.B.; supervision, G.S. and T.K.; project administration, G.S.; funding acquisition, G.S. All authors have read and agreed to the published version of the manuscript.

Funding: This work was supported by the Hungarian National Research, Development and Innovation Office (OTKA K119309 and K143550) and by the ÚNKP-21-4-SZTE-477 New National Excellence Program of the Ministry for Innovation and Technology from the source of the National Research, Development and Innovation Fund.

Institutional Review Board Statement: Not applicable.

Informed Consent Statement: Not applicable.

Data Availability Statement: Not applicable.

Conflicts of Interest: The authors declare no conflict of interest. The funders had no role in the design of the study; in the collection, analyses, or interpretation of data; in the writing of the manuscript; or in the decision to publish the results.

References

- Schumm, S.A. Geomorphic thresholds concept and its applications. *Trans. Inst. Br. Geogr.* **1979**, *4*, 485–515. [\[CrossRef\]](#)
- Gábris, G. A folyóvízi teraszok hazai kutatásának rövid áttekintése—A teraszok kialakulásának és korbeosztásának új magyarázata. *Földrajzi Közlemények* **2013**, *137*, 240–247.
- Starkel, L.; Michczyńska, D.J.; Gebica, P.; Kiss, T.; Panin, A.; Perşoiu, I. Climatic fluctuations reflected in the evolution of fluvial systems of Central-Eastern Europe (60–8 ka cal BP). *Quat. Int.* **2015**, *388*, 97–118. [\[CrossRef\]](#)
- Bulla, B. A Magyar medence pliocén es pleisztocén teraszai. *Földrajzi Közlemények* **1941**, *69*, 199–230.
- Pécsi, M. *A Magyarországi Duna-Völgy Kialakulása és Felszínalakítása*; Akadémiai Kiadó: Budapest, Hungary, 1959; p. 346.
- Vandenberghe, J. Timescales, climate and river development. *Quat. Sci. Rev.* **1995**, *14*, 631–638. [\[CrossRef\]](#)
- Gábris, G. A magyarországi folyóteraszok kialakulásának és korbeosztásának magyarázata az oxigénizotóp sztratigráfia tükrében. *Földrajzi Közlemények* **2006**, *130*, 123–133.
- Starkel, L.; Gebica, P.; Superson, J. Last Glacial–Interglacial cycle in the evolution of river valleys in southern and central Poland. *Quat. Sci. Rev.* **2007**, *26*, 2924–2936. [\[CrossRef\]](#)
- Schumm, S.A.; Dumont, J.F.; Holbrook, J.M. *Active Tectonics and Alluvial Rivers*; Cambridge University Press: Cambridge, UK, 2002; p. 276.
- Necea, D.; Fielitz, W.; Matenco, L. Late Pliocene–Quaternary tectonics in the frontal part of the SE Carpathians: Insights from tectonic geomorphology. *Tectonophysics* **2005**, *410*, 137–156. [\[CrossRef\]](#)
- Vandenberghe, J.; Wang, X.; Lu, H. Differential impact of small-scaled tectonic movements on fluvial morphology and sedimentology (the Huang shui catchment, NE Tibet Plateau). *Geomorphology* **2011**, *134*, 171–185. [\[CrossRef\]](#)
- Pécsi, M. *A Dunai Alföld*; Akadémia Kiadó: Budapest, Hungary, 1967.
- Ruszkiczay-Rüdiger, Z.; Fodor, L.; Bada, G.; Leel-Össy, S.; Horváth, E.; Dunai, T.J. Quantification of Quaternary vertical movements in the central Pannonian Basin: A review of chronologic data along the Danube River, Hungary. *Tectonophysics* **2005**, *410*, 157–172. [\[CrossRef\]](#)
- Bulla, B. Folyóterasz-problémák. *Földrajzi Közlemények* **1956**, *80*, 121–141.
- Schanz, S.A.; Montgomery, D.R.; Collins, B.D.; Duvall, A.R. Multiple paths to straths: A review and reassessment of terrace genesis. *Geomorphology* **2018**, *312*, 12–23. [\[CrossRef\]](#)
- Scherler, D.; Bookhagen, B.; Wulf, H.; Preusser, F.; Strecker, M.R. Increased late Pleistocene erosion rates during fluvial aggradation in the Garhwal Himalaya, northern India. *Earth Planet. Sci. Lett.* **2015**, *428*, 255–266. [\[CrossRef\]](#)
- Dey, S.; Thiede, R.C.; Schildgen, T.F.; Wittmann, H.; Bookhagen, B.; Scherler, D.; Jain, V.; Strecker, M.R. Climate-driven sediment aggradation and incision since the late Pleistocene in the NW Himalaya, India. *Earth Planet. Sci. Lett.* **2016**, *449*, 321–331. [\[CrossRef\]](#)
- Malatesta, L.C.; Avouac, J.-P. Contrasting river incision in north and south Tian Shan piedmonts due to variable glacial imprint in mountain valleys. *Geology* **2018**, *6*, 659–662. [\[CrossRef\]](#)
- Kiss, T.; Hernesz, P.; Sümeghy, B.; Györgyövcics, K.; Sipos, G. The evolution of the Great Hungarian Plain fluvial system—Fluvial processes in a subsiding area from the beginning of the Weichselian. *Quat. Int.* **2015**, *388*, 142–155. [\[CrossRef\]](#)
- Bendefy, L. A Maros geomorfológiája, Az Erdélyi-medence mai vízrendszerének földtani kialakulása. In *Vízrajzi Atlasz Sorozat 19. kötet. Maros 1. Fejezet. Hidrográfia, Geomorfológia*; Csoma, J., Laczay, I., Eds.; Országos Vízügyi Főigazgatóság: Budapest, Hungary, 1975; pp. 13–14.
- Berec, B.; Gábris, G. A Maros hordalékkúp bánási szakasza. In *Kárpát-Medence: Természet, Társadalom, Gazdaság (Földrajzi Tanulmányok)*; Frisnyák, S., Gál, A., Eds.; Nyíregyházi Főiskola Turizmus és Földrajztudományi Intézet; Hajdúböszörményi Bocskai István Gimnázium: Nyíregyháza, Hungary, 2013; pp. 51–64.
- Molnár, B. A Maros folyó kialakulása és vízgyűjtő területének földtani felépítése. *Hidrológiai Közöny* **2007**, *87*, 27–30.
- Sawicki, L.M. Pryczynki do morfologii Seidemiogrodu.—Beiträge zur Morphologie Siebenbürgens. In *Bulletin International De L'académie des Sciences*; Impimerie De L'université: Kraków, Poland, 1912.
- Pávai Vajna, F. A Maros-völgy kalakulásáról. *Földtani Közöny* **1914**, *44*, 256–280.
- Popp, N. Valea hunedoreană a Mureşului. *Lucr. Şt. Inst. Ped. Oradea, seria A. Geografie, Ed; Intitulul de Invatamint Superior din Ordadea, Ordadea, Romania*, 1977; 171–178.

26. Mike, K. *Magyarország Ősrajza és Felszíni Vizeinek Története*; Aqua Kiadó: Budapest, Hungary, 1991; pp. 361–577.
27. Braumann, S.M.; Neuhuber, S.; Fiebig, M.; Schaefer, J.M.; Hintersberger, E.; Lüthgens, C. Challenges in constraining ages of fluvial terraces in the Vienna Basin (Austria) using combined isochron burial and pIRIR₂₂₅ luminescence dating. *Quat. Int.* **2019**, *509*, 87–102. [[CrossRef](#)]
28. Zhang, J.-F.; Qiu, W.-L.; Hu, G.; Zhou, L.-P. Determining the Age of Terrace Formation Using Luminescence Dating—A Case of the Yellow River Terraces in the Baode Area, China. *Methods Protoc.* **2020**, *3*, 17. [[CrossRef](#)]
29. Jain, M.; Murray, A.S.; Bøtter-Jensen, L. Optically stimulated luminescence dating: How significant is incomplete light exposure in fluvial environments. *Quaternaire* **2004**, *15*, 143–157. [[CrossRef](#)]
30. Tóth, O.; Sipos, G.; Kiss, T.; Bartyik, T. Variation of OSL residual doses in terms of coarse and fine grain modern sediments along the Hungarian section of the Danube. *Geochronometria* **2017**, *44*, 319–330. [[CrossRef](#)]
31. Anechitei-Deacu, V.; Timar-Gabor, A.; Constantin, D.; Trandafir-Antohei, O.; Valle, L.; Fornós, J.; Gómez-pujol, L.; Wintle, A. Assessing the maximum limit of SAR-OSL dating using quartz of different grain sizes. *Geochronometria* **2018**, *45*, 146–159. [[CrossRef](#)]
32. Konecsny, K.; Bálint, G. Low water related hydrological hazards along the lower Mures/Maros River. *Riscuri Si Catastr.* **2009**, *8*, 202–207.
33. Katona, O.; Sipos, G.; Onaca, A.; Ardelean, F. Reconstruction of palaeo-hydrology and fluvial architecture at the Orosháza palaeo-channel of River Maros, Hungary. *J. Environmental Geogr.* **2012**, *5*, 29–38. [[CrossRef](#)]
34. Bartyik, T.; Sipos, G.; Filyó, D.; Kiss, T.; Urdea, P.; Timofte, F. Temporal relationship of increased palaeodischarges and Late Glacial deglaciation phases on the catchment of River Maros/Mureş, Central Europe. *J. Environ. Geogr.* **2021**, *14*, 39–46. [[CrossRef](#)]
35. Ianovici, V.; Borcoş, M.; Bleahu, M.; Patrulius, D.; Lupu, M.; Dimitrescu, R.; Savu, H. *Geologia Munților Apuseni*; Edit. Academiei: Bucharest, Romania, 1976; 630p.
36. Gheorghiu, C.; Calotă, C.; Zborea, A.; Mareş, I. *Aspecte Tectonice ale Culoarului Mureşului, Asoc.geol. carp.-balc.*; Congresul, V., Ed.; Carpatho-Balkan Geological Association: Bucharest, Romania, 1963; pp. 85–102.
37. Zugrăvescu, D.; Polonic, G.; Horomnea, M.; Dragomir, V. Recent vertical crustal movements on the Romanian territory, the major tectonic compartments and their relative dynamics. *Rev. Roum. Géophysique* **1998**, *42*, 3–14.
38. Mauz, B.; Bode, T.; Mainz, E.; Blanchard, H.; Hilger, W.; Dikau, R.; Zöller, L. The luminescence dating laboratory at the University of Bonn: Equipment and procedures. *Anc. TL* **2002**, *20*, 53–61.
39. Sipos, G.; Kiss, T.; Tóth, O. Constraining the age of floodplain levels along the lower section of river Tisza, Hungary. *J. Environ. Geogr.* **2016**, *9*, 39–44. [[CrossRef](#)]
40. Olley, J.; Caitcheon, G.; Murray, A. The distribution of apparent dose as determined by optically stimulated luminescence in small aliquots of fluvial quartz: Implications for dating young sediments. *Radiat. Meas.* **1998**, *30*, 207–217. [[CrossRef](#)]
41. Wintle, A.G.; Murray, A.S. A review of quartz optically stimulated luminescence characteristics and their relevance in single-aliquot regeneration dating protocols. *Radiat. Meas.* **2006**, *41*, 369–391. [[CrossRef](#)]
42. Galbraith, R.F.; Roberts, R.G. Statistical aspects of equivalent dose and error calculation and display in OSL dating: An overview and some recommendations. *Quat. Geochronol.* **2012**, *11*, 1–27. [[CrossRef](#)]
43. Arnold, L.J.; Bailey, R.M.; Tucker, G.E. Statistical treatment of fluvial dose distributions from southern Colorado arroyo deposits. *Quat. Geochronol.* **2007**, *2*, 162–167. [[CrossRef](#)]
44. Kreuzer, S.; Schmidt, C.; Fuchs, M.C.; Dietze, M.; Fischer, M.; Fuchs, M. Introducing an R package for luminescence dating analysis. *Anc. TL* **2012**, *30*, 1–8.
45. Jain, M.; Murray, A.S.; Bøtter-Jensen, L. Characterisation of blue light stimulated luminescence components in different quartz samples: Implications for dose measurement. *Radiat. Meas.* **2003**, *37*, 441–449. [[CrossRef](#)]
46. Durcan, J.A.; Duller, G.A.T. The fast ratio: A rapid measure for testing the dominance of the fast component in the initial OSL signal from quartz. *Radiat. Meas.* **2011**, *46*, 1065–1072. [[CrossRef](#)]
47. Gray, H.J.; Jain, M.; Sawakuchi, A.O.; Mahan, S.A.; Tucker, G.E. Luminescence as a sediment tracer and provenance tool. *Rev. Geophys.* **2019**, *57*, 987–1017. [[CrossRef](#)]
48. Bartyik, T.; Magyar, G.; Filyó, D.; Tóth, O.; Blanka-Végi, V.; Kiss, T.; Marković, S.; Persoiu, I.; Gavrilov, M.; Mezősi, G.; et al. Spatial differences in the luminescence sensitivity of quartz extracted from Carpathian Basin fluvial sediments. *Quat. Geochronol.* **2021**, *64*, 101166. [[CrossRef](#)]
49. Liritzis, I.; Stamoulis, K.; Papachristodoulou, C.; Ioannides, K. A re-valuation of radiation dose-rate conversion factors. *Mediterr. Archaeol. Archaeom.* **2013**, *13*, 1–15.
50. Prescott, J.R.; Hutton, J.T. Cosmic ray contributions to dose rates for luminescence and ESR dating: Large depths and long term variations. *Radiat. Meas.* **1994**, *23*, 497–500. [[CrossRef](#)]
51. Alexanderson, H. Residual OSL signals from modern Greenlandic river sediments. *Geochronometria* **2007**, *26*, 1–9. [[CrossRef](#)]
52. Marković, S.B.; Fitzsimmons, K.E.; Sprafke, T.; Gavrilović, D.; Smalley, I.J.; Jović, V.; Svirčev, Z.; Gavrilov, M.B.; Bešlin, M. The history of Danube loess research. *Quaternary. Int.* **2016**, *399*, 86–99. [[CrossRef](#)]
53. Van Huissteden, K.; Vandenberghe, J.; Pollard, D. Palaeotemperature reconstructions of the European permafrost zone during marine oxygen isotope Stage 3 compared with climate model results. *J. Quat. Sci.* **2003**, *18*, 453–464. [[CrossRef](#)]
54. Feurdean, A.; Perşoiu, A.; Taşău, I.; Stevens, I.; Magyari, E.K.; Onac, B.P.; Marković, S.; Andrić, M.; Connor, S.; Fărcaş, S.; et al. Climate variability and associated vegetation response through Central and Eastern Europe (CEE) between 60 and 8 ka. *Quat. Sci. Rev.* **2014**, *106*, 206–224. [[CrossRef](#)]

55. Van Meerbeeck, C.J.; Renssen, H.; Roche, D.M. How did Marine Isotope Stage 3 and Last Glacial Maximum climates differ?—Perspectives from equilibrium simulations. *Clim. Past* **2009**, *5*, 33–51. [[CrossRef](#)]
56. Cunha, P.P.; Martins, A.A.; Buylaert, J.-P.; Murray, A.S.; Gouveia, M.P.; Font, E.; Pereria, T.; Figueirido, S.; Ferreira, C.; Bridgland, D.R.; et al. The lowermost Tejo River terrace at foz do enxarrique, Portugal: A paleoenvironmental archive from c. 60–35 ka and its implications for the last neanderthals in Westernmost Iberia. *Quaternary* **2019**, *2*, 3. [[CrossRef](#)]
57. Winsemann, J.; Lang, J.; Roskosch, J.; Polom, U.; Böhner, U.; Brandes, C.; Glotzbach, C.; Frechen, M. Terrace styles and timing of terrace formation in the Weser and Leine valleys, northern Germany: Response of a fluvial system to climate change and glaciation. *Quat. Sci. Rev.* **2015**, *123*, 31–57. [[CrossRef](#)]
58. Olszak, J.; Kukulak, J.; Alexanderson, H. Revision of river terrace geochronology in the Orawa-Nowy Targ Depression, south Poland: Insights from OSL dating. *Proc. Geol. Assoc.* **2016**, *127*, 595–605. [[CrossRef](#)]
59. Vassallo, R.; Ritz, J.-F.; Braucher, R.; Jolivet, M.; Carretier, S.; Larroque, C.; Chauvet, A.; Sue, C.; Todbileg, M.; Bourlès, D.; et al. Transpressional tectonics and stream terraces of the Gobi-Altay, Mongolia. *Tectonics* **2007**, *26*, TC5013. [[CrossRef](#)]
60. Picotti, V.; Pazzaglia, F.J. A new active tectonic model for the construction of the Northern Apennines mountain front near Bologna (Italy). *J. Geophys. Res. Solid Earth* **2008**, *113*, B08412. [[CrossRef](#)]
61. Fuller, T.K.; Perg, L.A.; Willenbring, J.K.; Lepper, K. Field evidence for climate-driven changes in sediment supply leading to strath terrace formation. *Geology* **2009**, *37*, 467–470. [[CrossRef](#)]
62. Antoine, P.; Lautridou, J.P.; Laurent, M. Long-term fluvial archives in NW France: Response of the seine and Somme rivers to tectonic movements, climatic variations and sea-level changes. *Geomorphology* **2000**, *33*, 183–207. [[CrossRef](#)]
63. Vandenberghe, J. The fluvial cycle at cold-warm-cold transitions in lowland regions: A refinement of theory. *Geomorphology* **2008**, *98*, 275–284. [[CrossRef](#)]
64. Gábris, G.; Horváth, E.; Novothny, Á.; Ruzsiczay-Rüdiger, Z. Fluvial and aeolian landscape evolution in Hungary—results of the last 20 years research. *Netherland J. Geosci.* **2012**, *91*, 111–128. [[CrossRef](#)]
65. Bridgland, D.R. The Middle and Upper Pleistocene sequence in the Lower Thames: A record of Milankovitch climatic fluctuation and early human occupation of southern Britain. *Proc. Geol. Assoc.* **2006**, *117*, 281–305. [[CrossRef](#)]
66. Yang, H.; Yang, X.; Huang, W.; Li, A.; Hu, Z.; Huang, X.; Yang, H. ¹⁰Be and OSL dating of Pleistocene fluvial terraces along the Hongshuiba River: Constraints on tectonic and climatic drivers for fluvial downcutting across the NE Tibetan Plateau margin, China. *Geomorphology* **2020**, *348*, 106884. [[CrossRef](#)]
67. Urdea, P.; Onaca, A.; Ardelean, M.; Ardelean, M. New Evidence on the Quaternary Glaciation in the Romanian Carpathians, cap. 24. In *Quaternary Glaciations—Extent and Chronology. A Closer Look*; Ehlers, J., Gibbard, P.L., Hughes, P.D., Eds.; Elsevier: Amsterdam, The Netherlands, 2011; pp. 305–322. [[CrossRef](#)]
68. Ruzsiczay-Rüdiger, Z.; Kern, Z.; Urdea, P.; Braucher, R.; Madarász, B.; Schimmelpfennig, I. Revised deglaciation history of the Pietrele-Stânișoara glacial complex, Retezat Mts, Southern Carpathians, Romania. *Quat. Int.* **2011**, *415*, 216–229. [[CrossRef](#)]
69. Ruzsiczay-Rüdiger, Z.; Kern, Z.; Urdea, P.; Madarász, B.; Braucher, R. ASTER TEAM Limited glacial erosion during the last glaciation in mid-latitude cirques (Retezat Mts, Southern Carpathians, Romania). *Geomorphology* **2011**, *384*, 107719. [[CrossRef](#)]
70. Pazzaglia, F.J. Fluvial terraces. In *Treatise on Geomorphology*; Elsevier: Amsterdam, The Netherlands, 2013; pp. 379–412. [[CrossRef](#)]
71. Kiss, T.; Sümegehy, B.; Sipos, G. Late Quaternary paleo-drainage reconstruction of the Maros River Alluvial Fan. *Geomorphology* **2014**, *204*, 49–60. [[CrossRef](#)]
72. Kasse, C.; Hoek, W.Z.; Bohncke, S.J.P.; Konert, M.; Weijers, J.W.H.; Cassee, M.L.; Van der Zee, R.M. Late Glacial fluvial response of the Niers-Rhine (western Germany) to climate and vegetation change. *J. Quat. Sci.* **2005**, *20*, 377–394. [[CrossRef](#)]
73. Necea, D.; Fielitz, W.; Kadereit, A.; Andriessen, P.A.M.; Dinu, C. Middle Pleistocene to Holocene fluvial terrace development and uplift-driven valley incision in the SE Carpathians, Romania. *Tectonophysics* **2013**, *602*, 332–354. [[CrossRef](#)]
74. Van Balen, R.T.; Houtgast, R.F.; Van der Wateren, F.M.; Vandenberghe, J.; Bogaart, P.W. Sediment budget and tectonic evolution of the Meuse catchment in the Ardennes and the Roer Valley rift system. *Glob. Planet. Chang.* **2000**, *27*, 113–129. [[CrossRef](#)]
75. Gunnell, Y.; Gallagher, K.; Carter, A.; Widdowson, M.; Hurford, A.J. Denudation history of the continental margin of western peninsular India since the early Mesozoic; reconciling apatite fission-track data with geomorphology. *Earth Planet. Sci. Lett.* **2003**, *215*, 187–201. [[CrossRef](#)]
76. Pan, B.; Wu, G.; Wang, Y.; Liu, Z.; Guan, Q. Ages and genesis of the Shangou River terraces in eastern Qilian Mountains. *Chin. Sci. Bull.* **2001**, *46*, 510–515. [[CrossRef](#)]
77. Tofelde, S.; Schildgen, T.F.; Savi, S.; Pingel, H.; Wickert, A.D.; Bookhagen, B.; Wittmann, H.; Alonso, R.N.; Cottle, J.; Strecker, M.R. 100 kyr fluvial cut-and-fill terrace cycles since the Middle Pleistocene in the southern Central Andes, NW Argentina. *Earth Planet. Sci. Lett.* **2017**, *473*, 141–153. [[CrossRef](#)]
78. Bartyik, T. Reconstruction of Fluvial Processes in the Maros River Basin, with Particular Reference to the Applicability of OSL Sensitivity. Ph.D. Thesis, University of Szeged, Szeged, Hungary, 2022.

Disclaimer/Publisher’s Note: The statements, opinions and data contained in all publications are solely those of the individual author(s) and contributor(s) and not of MDPI and/or the editor(s). MDPI and/or the editor(s) disclaim responsibility for any injury to people or property resulting from any ideas, methods, instructions or products referred to in the content.